THEORETICAL STUDIES OF HYDRIDE TRANSFER REACTIONS

SEBASTIÃO J. FORMOSINHO

Departamento de Química, Universidade de Coimbra, 3049 Coimbra Codex, Portugal

The intersecting-state model (ISM) has been applied to the study of hydride transfer reactions between variously substituted and elaborated pyridinium ions in solution. Chemical bond order is conserved along the reaction coordinate, with a transition state bond order of $n^+ = 0.5$. This supports the view that these reactions have essentially a synchronous nature and occur by thermal activation over an energy barrier. Tunnelling of H^- is negligible because the effective mass for the solvated species is high. Reaction energy and kinetic isotope effects are well accounted for by the model. For reactions in the vapour phase, ISM and the tunnel effect theory show that tunnelling becomes the dominant mechanism. The same is also valid for proton transfers in the vapour phase.

INTRODUCTION

Most commonly, hydrogen is transferred as a proton between atoms with available electron pairs. The alternative hydride transfer is a closed shell process, because it can be considered as the transfer of a proton with a pair of electrons between electron-deficient sites:

$$A_i^n + A_j H^m \rightarrow A_i H^{n-1} + A_j^{m+1} \qquad (1)$$
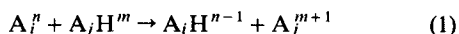
Owing to the importance of the last category of reactions in organic and biological chemistry, the field has been reviewed frequently[1,2] and a large number of theoretical studies based on intersecting-state models (ISMs) have been addressed to this topic.[3] In general, Marcus theory[4] gives a reasonably accurate representation of the relationship between rate and equilibrium constants for reactions of type (1). Nevertheless, none of those studies answers the interesting question of why the intrinsic kinetic energy barriers, $\Delta G^{\pm}$, are so high for hydride transfers. According to Kreevoy and Truhlar,[3d] semiempirical rate theory cannot answer this question and, in fact, deliberately tries to avoid it, the answer being obtainable from quantum mechanical calculations. Further, much effort has been devoted to distinguishing between the concerted or stepwise character of reactions (1) and to assess the role of tunnelling in these processes.[3c]

The recently developed ISM[5] appears to be more general than other semiempirical one-dimensional models of chemical reactivity;[3f] in particular, it encompasses the theory of Marcus and the BEBO model as particular cases.[5,6] Further, it has provided a better understanding of proton transfer reactions in either ground[7] or excited states[3f,8] than these other models. Owing to the

similarity of proton and hydride transfer reactions, it appears feasible to apply ISM to the study of the latter processes to try to answer some of the above questions.

THE INTERSECTING-STATE MODEL

The classical ISM of harmonic oscillators has been described in detail elsewhere,[5–8] and only the essential features will be presented here. The model represents the potential energy curves for reactant and products by parabolas (of force constants, f), displaced vertically by the reaction energy, ΔG^0, and horizontally by the sum of the bond extensions of reactant and product to the transition state, d. One can then write the equality

$$(1/2)f_r x^2 = (1/2)f_p(d-x)^2 + \Delta G^0 \qquad (2)$$

and solve for the reactant bond extension, x, to determine the activation free energy:

$$\Delta G^+ = (1/2)f_r x^2 \qquad (3)$$

We have shown[5] that d is proportional to the sum of the equilibrium bond lengths of reactant and product:

$$d = \eta(l_r + l_p) \qquad (4)$$

where the reduced bond extension η is given by

$$\eta = \frac{a' \ln 2}{n^+} + \frac{a'}{2\lambda^2}(\Delta G^0)^2 \qquad (5)$$

n^+ is the transition-state bond order, λ is an energy parameter which measures the capacity of the transition state to accommodate energy and a' is a constant found empirically to be $a' = 0.156$.[5] The rate constants can now be calculated by transition state theory:

$$k = (k_B T/h)C_0^{1-m} \exp(-\Delta G^+/RT) \qquad (6)$$

where C_0 is the standard concentration ($C_0 = 1$ M) and m is the molecularity of the reaction; in the present case, $m = 2$.

For bond-forming–bond-breaking processes of single bonds, conservation of the bond order at the transition state leads to

$$n_r^{\ddagger} + n_p^{\ddagger} = 1 \qquad (7)$$

and for the thermoneutral situation $n_r^{\ddagger} = n_p^{\ddagger} = n^{\ddagger} = 0.5$. In bond-forming–bond-breaking processes of single bonds involving electron-rich sites, the total bond order is not conserved at the transition state and $n^{\ddagger} > 1/2$.[5,6,9] For example, we have shown[7a] that for proton transfer reactions in water $0.5 < n^{\ddagger} < 1$, $n^{\ddagger}$ being close to 0.5 for carbon acids and close to 1 for HF.

Obviously, if quantum-mechanical tunnelling overcomes thermal activation, one expects that the empirical value of $n^{\ddagger}$ will be larger than 0.5 for cases where the bond order is conserved; for reactions where the total bond order is not conserved, $n^{\ddagger}$ will be higher than its maximum possible value, compatible with the electronic characteristics of the reactive sites.[9] In contrast, the loss of the concerted character of the reaction will lead to $n^{\ddagger} < 0.5$ (or the maximum value).[10-12]

RESULTS AND DISCUSSION

Reactions in solution

Kreevoy and Lee[3b] studied the hydride transfer reactions between nicotinamide adenine dinucleotide (NAD^+) analogues in isopropyl alcohol–water (20%) mixtures:

$$(8)$$
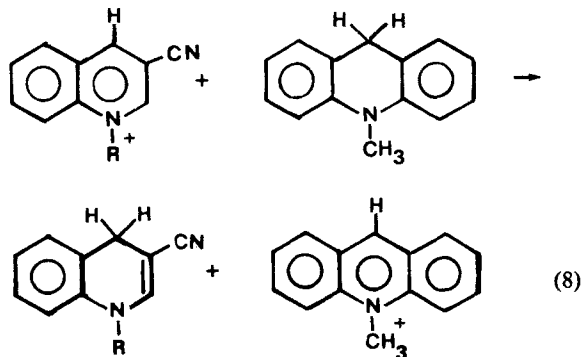
They proposed a modification of the Marcus equation which attempts to take into consideration variations in bond order through a parameter τ related to the charge, δ, on the in-flight H($1 - \tau = \delta$ for proton transfer[3f] and $\tau - 1 = \delta$) for hydride transfers[3b] and substitution effects perpendicular to the reaction coordinate. The

energy barrier is given by

$$\Delta G^{\ddagger} = \frac{\lambda_M}{4} + \frac{\Delta G^0}{2} + \frac{(\Delta G^0)^2}{4\lambda_M} + \frac{(\tau - 1)}{2} \Delta G^0 \qquad (9)$$

where λ_M is the well known reorganization parameter of the theory of Marcus.[4] The Brønsted coefficient α is

$$\alpha = \frac{\partial \Delta G^{\ddagger}}{\partial \Delta G^0} = \chi + \frac{\tau - 1}{2} \qquad (10)$$

where χ represents the degree of atom or ion transfer at the transition state along the diagonal of an Albery–Jencks–More O'Ferrall diagram.[3b] These studies lead to a total transition state bond order $\tau = 0.77$.

Although χ corresponds to x/d of our model,[3f] there are considerable differences between Kreevoy's model and ISM. Whereas the former model, like other theoretical models which generalize Marcus–BEBO theories,[13] adds a second coordinate to the single reaction coordinate of the theory of Marcus, ISM considers only a single coordinate. Further, it easily incorporates the asymmetry of the potential energy with $f_r \neq f_p$, whereas Marcus models are essentially symmetric, $f_r = f_p$. Another very important difference is the dependence of $\Delta G^{\ddagger}$ on ΔG^0; compare equation (9) with the dependence implicit in the ISM model[14]:

$$\Delta G^{\ddagger} = c_0 + c_1 \Delta G^0 + c_2 (\Delta G^0)^2 \\ + c_4 (\Delta G^0)^4 + c_6 (\Delta G^0)^6 + \cdots \qquad (11)$$

where c_i are coefficients independent of ΔG^0.

For the hydride transfer reactions in equation (8) the reactive bonds are the CH bonds (sp^3). Data for the force constants and bond lengths were taken from Ref. 15, giving typical values for organic compounds, $f_r = f_p = 2.9 \times 10^3$ kJ mol^{-1} Å^{-2} and $l = l_r + l_p = 2.192$ Å. The energy barriers were estimated from rate constant data[3b] through equation (6) ($T = 298$ K) and subsequently equations (3), (2) and (5) allow the estimation of x, d and η as presented in Table 1. Figure 1 illustrates that for the majority of the reactions there is a square dependence of η on ΔG^0, according to equation (5). From Figure 1, the intercept leads to $\eta_0 = 0.2195 \pm 0.0005$ and $\lambda = 86 \pm 5$ kJ mol^{-1}; equation (5) allows also the estimation of $n^{\ddagger} = 0.492 \pm 0.001$.

The transition state bond order is extremely close to 0.5, implying, in contrast with the findings of Kreevoy and Lee,[3b] that there is conservation of the total bond order. Further, such values imply that hydride transfer reactions of equation (8) are virtually concerted and synchronous processes and that H-tunnelling is negligible. The solvation of the $H^{\delta-}$ species increases the effective mass and quantum mechanical tunnelling cannot compete with thermal activation for hydride transfers in solutions, as will be discussed later.

Within ISM, the intrinsic energy barrier is

$$\Delta G_0^{\ddagger} = (1/8) f [(a' \ln 2/n^{\ddagger})(l_r + l_p)]^2 \qquad (12)$$

Table 1. Reduced bond extensions of hydride transfers of quinolinium ions [equation (8)] [a]

R	$\Delta G^{\ddagger}$/kJ mol^{-1} [b]	ΔG^0/kJ mol^{-1} [b]	d/Å	η
a p-CH$_3$C$_6$H$_4$CH$_2$	80·9	− 6·8	0·4821	0·2199
b C$_6$H$_5$CH$_2$	80·6	− 7·6	0·4825	0·2201
c p-FC$_6$H$_4$CH$_2$	80·5	− 8·1	0·4828	0·2202
d m-B$_r$C$_6$H$_4$CH$_2$	80·0	− 9·1	0·4828	0·2202
e m-FC$_6$H$_4$CH$_2$	79·6	− 9·4	0·4821	0·2199
f p-CNC$_6$H$_4$CH$_2$	79·5	− 10·9	0·4838	0·2207
g m-CF$_3$C$_6$H$_4$CH$_2$	79·0	− 11·7	0·4835	0·2206
h p-CF$_3$C$_6$H$_4$CH$_2$	79·5	− 8·1	0·4798	0·2190
i CH$_3$	84·8	2·8	0·4797	0·2188

[a] $f_r = f_p = 2\cdot9 \times 10^3$ kJ mol^{-1} Å^{-2}, $l_r + l_p = 2\cdot192$ Å.
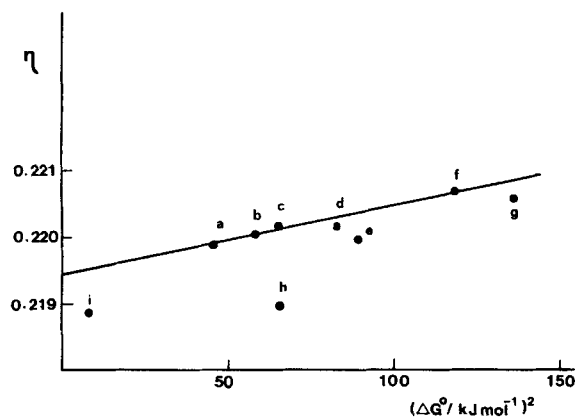[b] Ref. 3b, 298 K.

Figure 1. Plot of η versus $(\Delta G^0)^2$ for hydride transfers of quinolinium ions. Legend for reactions (a–i) in Table 1

This expression interprets the high $\Delta G_0^{\ddagger}$ for hydride transfer reactions as being due to the low $n^{\ddagger}$ ($n^{\ddagger} = 0\cdot5$), because H$^-$ transfer occurs essentially between electron-deficient sites. Notwithstanding, weak charge-transfer effects can be present in these reactions.

It is interesting that some symmetry-allowed sigmatropic shifts may assume hydridic character.[1] The application of ISM to shift reactions of hexa-1,5-dienes

also leads to $n^{\ddagger} = 0\cdot5$; nevertheless, $n^{\ddagger}$ can be increased by the presence of electron-rich substituents.[10]

The effect of substituents on $n^{\ddagger}$ has also been found in several proton transfer reactions, where $n^{\ddagger}$ increases with a decrease in the ionization energy of the reactants.[16] Charge-transfer effects present in H$^-$ transfers can be responsible for some scatter in the data in Figure 1. For symmetric hydride transfer reactions between aromatic molecules, with $\Delta G^0 = 0$, such effects are particularly notorious. The rates[3g] are higher for the larger ring systems and $n^{\ddagger}$ increases with a decrease in the ionization energy of the aromatic molecules (Table 2). Nevertheless, the values of $n^{\ddagger}$ are close to 0·5 (0·5–0·47).

The value of $\lambda = 86$ kJ mol^{-1} is considerably smaller than those found in proton transfer reactions ($\lambda \geqslant 200$ kJ mol^{-1}) of comparable $n^{\ddagger}$ values.[7,8,19] This implies 'tighter' and/or less solvated transition states for hydride transfer. Previous studies[20] based on qualitative arguments from molecular orbital theory suggested that, because antibonding orbitals were not populated, the hydride transfer transition states are tighter than those of related proton transfers.

The low λ value also accounts for the relatively low Brønsted coefficients of these reactions.[7a] With the above-reported $n^{\ddagger}$ and λ values and the corresponding

Table 2. Transition-state bond orders for symmetrical hydride transfers with $\Delta G^0 = 0$ [a]

Compound	k/mol^{-1}dm^3 s^{-1} [b]	$\Delta G_0^{\ddagger}$/kJ mol^{-1}	$n^{\ddagger}$	I/eV
Acridine	$4\cdot3 \times 10^{-2}$	80·5	0·503	7·9[c]
Quinoline	$3\cdot1 \times 10^{-3}$	87·9	0·483	8·5[d]
Phenanthridine	$1\cdot1 \times 10^{-3}$	89·6	0·476	
Pyridine	$2\cdot3 \times 10^{-5}$	99·1	0·472	9·3[e]
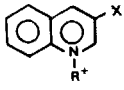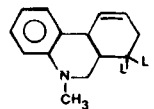
[a] $f = 2\cdot9 \times 10^3$ kJ mol^{-1} Å^{-2}, $l = 2\cdot192$ Å.
[b] Ref. 3g.
[c] Ref. 16.
[d] Ref. 17.
[e] Ref. 18.

Table 3. Reduced bond extensions for hydride transfer reactions between [structure] and [structure] (L = H or D)[a]

R	X	ΔG^0/kJ mol^{-1}[b]	$\Delta G^{\dagger}$/kJ mol^{-1}[b]		d/Å		η	
			H	D	H	D	H	D
a CH_3	$CONH_2$	$-16\cdot9$	$77\cdot4$	$81\cdot6$	$0\cdot4861$	$0\cdot4979$	$0\cdot2218$	$0\cdot2271$
b $CH_2C_6H_5$	$CONH_2$	$-20\cdot6$	$75\cdot1$	$79\cdot2$	$0\cdot4844$	$0\cdot4961$	$0\cdot2201$	$0\cdot2263$
c $CH_2C_6H_4pCN$	$CONH_2$	$-24\cdot7$	$73\cdot7$	$77\cdot8$	$0\cdot4860$	$0\cdot4975$	$0\cdot2217$	$0\cdot2270$
d $CH_2C_6H_4pCH_3$	CN	$-42\cdot7$	$68\cdot2$	$72\cdot1$	$0\cdot4934$	$0\cdot5042$	$0\cdot2251$	$0\cdot2300$
e $CH_2C_6H_5$	CN	$-43\cdot5$	$68\cdot0$	$71\cdot9$	$0\cdot4939$	$0\cdot5048$	$0\cdot2253$	$0\cdot2303$
f $CH_2C_6H_4pCN$	CN	$-46\cdot8$	$67\cdot4$	$71\cdot2$	$0\cdot4963$	$0\cdot5069$	$0\cdot2264$	$0\cdot2313$

[a] $f_r = f_p = 2\cdot9 \times 10^3$ kJ mol^{-1} Å^{-2}, $l_r + l_p = 2.192$ Å (see text).
[b] Ref. 3c, 298 K.

f and l data, a value of α between $0\cdot39$ and $0\cdot32$ is calculated for $\Delta G^0 = -6$ and -10 kJ mol^{-1}, respectively; the experimental value is close to 0.39. If the experimental energy region was more extended, curved Brønsted plots would be expected.

Kreevoy et al.[3c] also studied kinetic deuterium isotope (KIE) effects on hydride transfer reactions in solution. Based on dynamic theories of tunnelling, they concluded that because of the large curvature of the reaction paths, a 'cutting the corner' tunnelling process could be significant.
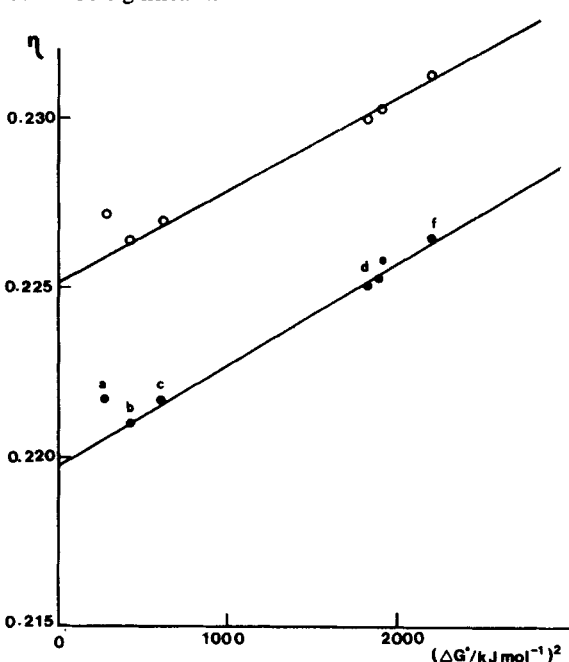

Figure 2. Plot of η versus $(\Delta G^0)^2$ for hydride transfer reactions presented in Table 3 (a–f). •, H transfer; ∘, D transfer

Table 3 shows the application of ISM to the study of those reactions and Figure 2 illustrates the expected linear dependence of η on $(\Delta G^0)^2$. These plots give the following set of values from the intercepts and slopes: $\eta_0(H) = 0\cdot220 \pm 5 \times 10^{-4}$, $\lambda(H) = 161$ kJ mol^{-1}, $\eta_0(D) = 0\cdot225 \pm 5 \times 10^{-4}$ and $\lambda(D) = 171$ kJ mol^{-1}. These sets of data [$\eta_0(H) = 0\cdot21972$; $\eta_0(D) = 0\cdot22525$] allow a reasonable account of the experimental KIE. As Figure 3 illustrates, such agreement is not possible when one neglects the square dependence of η on $\Delta G^0(\lambda \gg |\Delta G^0|)$.

The value of $\eta_0(H) = 0\cdot220$ leads to $n^* = 0\cdot492$, again supporting the view that these hydride transfers in solution are synchronous reactions which proceed, via thermal activation, over an energy barrier.

Kinetic isotope effect cannot be explained within a classical harmonic oscillator formalism. However, one can interpret, qualitatively, the different $\eta_0(H)$ and $\eta_0(D)$ values in terms of different effective bond lengths (ca $2\cdot5\%$ higher for CD) as being due to the more significant population, at room temperature, of excited vibrational modes ($v > 0$) for anharmonic CD modes. As discussed previously, ISM predicts curved Brønsted plots for hydride transfer reactions, as found experimentally.[3c] The calculated α values are $\alpha \approx 0\cdot4$ at $\Delta G^0 = 15$ kJ mol^{-1} and $\alpha \approx 0\cdot1$ at $\Delta G^0 = -50$ kJ mol^{-1}.

Although λ is higher for reactions in Table 3 than those in Table 1, it reveals again reasonably tight transition states. The parameter λ is slightly higher for the deuterated compounds owing to a mass effect. As found for hydrogen-atom transfer reactions, λ is small when in the transition state ABC† a light atom vibrates against two heavy atoms.[5]

Reactions in the vapour phase

Meot-Ner (Mautner) and Field[3e] have studied several hydride transfers between carbonium ions and several
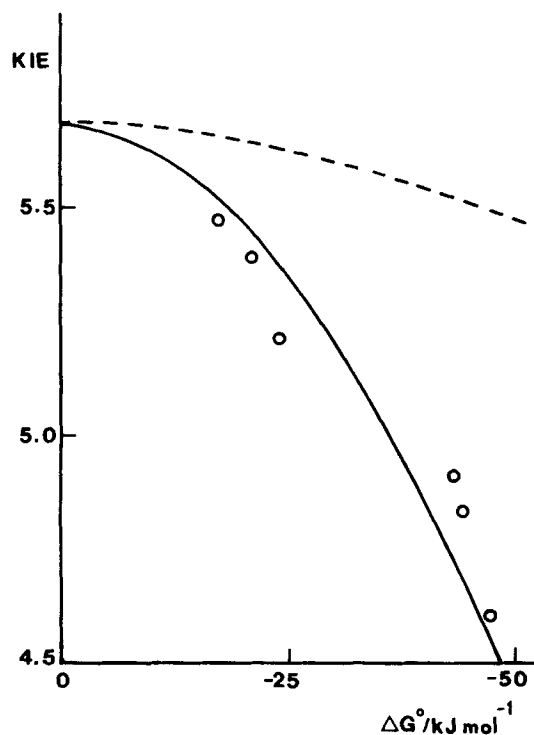
Figure 3. Calculated (solid line) kinetic isotope effects (KIE) for hydride transfer reactions in Table 3 as a function of ΔG^0 with $\eta_0(H) = 0.21972$, $\lambda(H) = 161$ kJ mol^{-1}, $\eta_0(D) = 0.22525$, $\lambda(D) = 171$ kJ mol^{-1}, $f = 2 \cdot 9 \times 10^3$ kJ mol^{-1} Å^{-2} and $l_r + l_p = 2.192$ Å. o, Experimental data; broken line, calculated KIE with $\lambda \gg |\Delta G^0|$
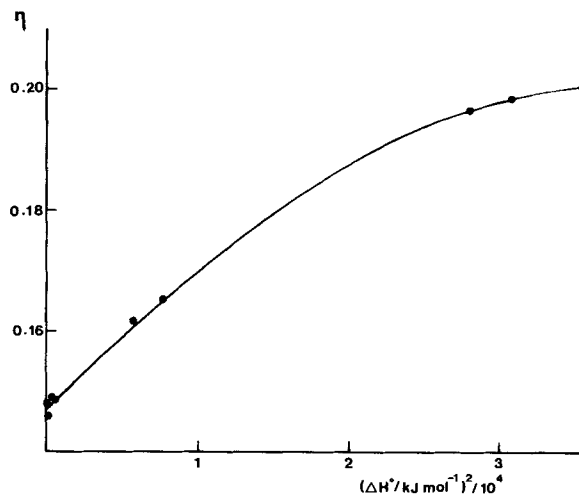

Figure 4. Plot of η versus $(\Delta H^0)^2$ for hydride transfers between carbonium ions and hydrocarbons in the vapour phase; calculated data in Table 4

hydrocarbons in the vapour phase. The reactions are considerably faster than in solution. Table 4 shows the results of the application of ISM to such experimental data, and Figure 4 presents the usual η versus $(\Delta G^0)^2$ plot, under the hypothesis that the reactions proceed via thermal activation. The first conclusion that one may draw from the intercept ($\eta_0 = 0 \cdot 147$) in Figure 4 is the

apparently high value of n^+ under the present assumptions, $n^+ = 0 \cdot 74$. As we have stated before, a value of $n^+ > 0 \cdot 5$ may well suggest that such reactions proceed via quantum mechanical tunnelling, in the vapour phase.

We have shown[21] that the potential energy barriers calculated by ISM are also adequate for assessing tunnelling mechanisms, through the tunnel effect theory (TET),[22] for adiabatic reactions:

$$k = AK_{pc} \exp - \{(2\pi/h)[2M\Delta G^*]\Delta x\} \qquad (13)$$

where A is a frequency factor taken typically as a CH frequency ($A = 10^{14}$ s^{-1}), K_{pc} is the constant of formation of the precursor complex, M is the tunnelling mass and Δx the barrier width; for $\Delta G^0 = 0$ $\Delta x = d$ and for $\Delta G^0 \neq 0$ $\Delta x = d - y$ with $y = (2\Delta G^0/f)^{1/2}$. Table 5 presents the calculated tunnelling rates [equation (13)] for the energy barriers estimated with $n^+ = 0 \cdot 49$, $f = 2 \cdot 9 \times 10^3$ kJ mol^{-1} Å^{-2}, $l = 2 \cdot 192$ Å and $M = 1$ g.

Table 4. Reduced bond extensions for hydride transfer between carbonium ions and hydrocarbons in the vapour phase, $R_1^+ + R_2H \rightarrow R_1H + R_2^{+a}$

R_1^+	R_2H	ΔG^*/kJ mol$^{-1 \, b}$	ΔH^0/kJ mol$^{-1 \, b}$	d/Å	η
⋏	⋏⋏	35·8	−5·4	0·3253	0·1486
⋏	⋏	30·2	−14·2	0·3194	0·1457
⋏	⋏⋏	29·8	−19·7	0·3280	0·1496
⋏	⋏	27·3	−22·6	0·3226	0·1472
⋏	⋏	15·6	−75·2	0·3542	0·1616
⋏	⋏	13·8	−87·8	0·3623	0·1653
$C_2H_5^+$	⋏	9·8	−167·2	0·4315	0·1969
$C_2H_5^+$	⋏	9·0	−175·6	0·4355	0·1987
$C_2H_5^+$	⋏⋏	7·5	−188·1	0·4392	0·2004

$^a f = 2 \cdot 9 \times 10^3$ kJ mol^{-1} Å^{-2}, $l = 2 \cdot 192$ Å.
^{b} Ref. 3e, 450 K.

Table 5. Rate constants for hydride transfer reactions in the vapour phase through quantum-mechanical tunnelling

	$k/l\ mol^{-1}\ s^{-1}$		Relative rates		
$\Delta H^0/kJ\ mol^{-1}$	Exp.[a]	Tun.[b]	Exp.	Tun.	KIE[c]
0	4×10^8	5×10^9	1	1	85
-80	2×10^{11}	2×10^{12}	500	400	65
-170	8×10^{11}	2×10^{13}	2000	4000	2·5

[a] Ref. 3e.
[b] Equation (13) with $K_{pc} = 1$.
[c] Effect of mass and $A(H)/A(D) = 1·36$.

Although the calculated rates are about an order of magnitude higher than experiment with $K_{pc} = 1$, the effect of reaction energy is well accounted for by tunnelling, in agreement with the suggestion of Kreevoy et al.,[3c] valid for tunnelling of an H^- species or tunnelling of an electron (pair) followed by tunnelling of an H (H^+) species. Owing to the dependence of the rates of tunnelling on the height and width of the reaction energy barrier [equation (13)], the k_{tun} values are more sensitive to ΔG^0 than the rates for thermal activation. In consequence, the plot in Figure 4 is no longer linear, but shows a downward curvature.

In liquid solutions, the presence of a 'solvated' ion such as H_3O^- drops the quantum mechanical tunnelling rate by nine orders of magnitude at $\Delta H^0 = 0$ ($k_{tun} = 5\ l\ mol^{-1}\ s^{-1}$), such that this cannot compete with thermal activation ($k_{therm} = 1·4 \times 10^3\ l\ mol^{-1}\ s^{-1}$).

The calculated KIEs for a tunnelling mechanism are considerably higher than those observed in solution, particularly when the reactions are not very exothermic (Table 5).

Table 6. Reduced bond extension for proton transfer reactions $t\text{-}C_4H_9^+ + M \rightarrow MH^+ + i\text{-}C_4H_8$ in the vapour phase[a]

M	$\Delta G^{\ddagger}/kJ\ mol^{-1}$ [b]	$\Delta G^0/kJ\ mol^{-1}$ [b]	η
1 $(i\text{-}C_3H_7)_2O$	5·2	$-43·1$	0·106
2 $(C_2H_5)_2CO$	4·8	$-23·4$	0·087
3 CH_3COOCH_3	5·7	$-10·5$	0·075
4 $CH_3COOC_2H_5$	5·3	$-20·9$	0·086
5 $(n\text{-}C_3H_7)_2O$	5·4	$-29·3$	0·095
6 $c\text{-}C_4H_6O$	5·7	$-15·9$	0·082
7 $HCOOC_4H_9$	9·0	1·7	0·069
8 $HCOOC_3H_7$	9·8	2·5	0·071

[a] $f_r = 2·9 \times 10^3$ kJ $mol^{-1}\ Å^{-2}$(CH), $f_p = 4·2 \times 10^3$ kJ $mol^{-1}\ Å^{-2}$ (MH), $l = 2·0$ Å.
[b] Ref. 23.
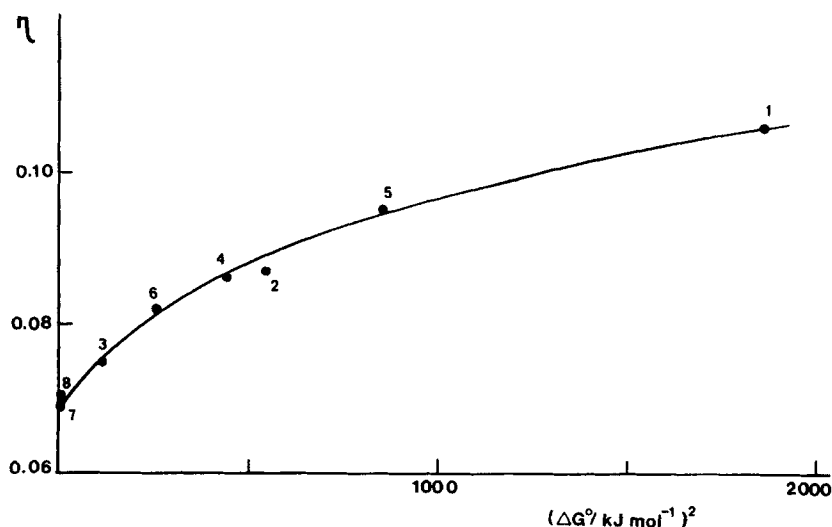
Figure 5. Plot of η versus $(\Delta G^0)^2$ for proton transfer reactions in the vapour phase, $t\text{-}C_4H_9^+ + M \rightarrow MH^+ + i\text{-}C_4H_8$; data in Table 6 (1–8)

Proton transfers in the vapour phase

It is interesting to see if the present findings for hydride transfer in the vapour phase are also verified for proton transfer reactions. A preliminary account of such a study has been presented.[12] Table 6 presents the ISM calculations and the plot in Figure 5, also showing a downward curvature, allows one to obtain $\eta_0 = 0\cdot069$ which corresponds to $n^\ddagger = 1\cdot56$, higher than the maximum expected value of $1\cdot0$; in fact, for oxygen acids in water $n^\ddagger \approx 0\cdot8$. With this value, $f_r = 2\cdot9 \times 10^3$ kJ mol^{-1}, $f_p = 4\cdot2 \times 10^3$ kJ mol^{-1} Å^{-2} and $l = 2\cdot0$ Å^{15} the calculated tunnelling rate constant, at $\Delta G^0 = 0$, is $k = 3 \times 10^{12}$ l mol^{-1} s^{-1}, which again is an order of magnitude higher than the experimental rate of 2×10^{11} l mol^{-1} s^{-1}. A better agreement is obtained with $K_{pc} \approx 0\cdot07$, as found also for hydride transfers.

CONCLUSIONS

We have shown that hydride transfer reaction in solution proceed via thermal activation over an energy barrier interpretable within the ISM formalism, with conservation of the transition-state bond order. This supports the synchronous character of such processes. In the vapour phase the rates are considerably higher owing to quantum mechanical tunnelling of H$^{\delta-}$ between two electron-deficient sites. In solution tunnelling cannot compete with thermal activation, because the tunnelling mass is considerably higher owing to the solvation of the H$^-$ species. Although proton transfer reactions in solution can be considerably faster than hydride transfers, owing to an increase in the transition-state bond order ($n^\ddagger > 0\cdot5$) from the available electron pairs of the reaction sites, in the vapour phase the rates appear also to be controlled by tunnelling through the reaction energy barrier.

REFERENCES

1. C. I. F. Watt, Adv. Phys. Org. Chem. 24, 57 (1988).
2. P. Ahlberg, G. Jonsäll and C. Engdahl, Adv. Phys. Org. Chem. 19, 223 (1983); L. Eberson, Adv. Phys. Org. Chem. 18, 79 (1982).
3. (a) L. Eberson, Acta Chem. Scand., Ser. B 38, 439 (1984); (b) M. M. Kreevoy and I. S. H. Lee, J. Am. Chem. Soc. 106, 2550 (1984); (c) M. M. Kreevoy, D. Ostović, D. G. Truhlar and B. C. G. Garrett, J. Phys. Chem. 90, 3766 (1986); (d) M. M. Kreevoy and D. G. Truhlar, in Rates and Mechanisms of Reactions, edited by C. F. Bernasconi, 4th ed. Chap. 1. Wiley, New York (1986); (e) M. Meot-Ner (Mautner) and F. H. Field, J. Am. Chem. Soc. 100, 1356 (1978); (f) K. Yates, J. Phys. Org. Chem. 2, 300 (1989); (g) M. M. Kreevoy, D. Ostovic, I.-S.H. Lee, D. A. Binder and G. W. King, J. Am. Chem. Soc. 110, 524 (1988).
4. R. A. Marcus, J. Phys. Chem. 72, 891 (1968).
5. A. J. C. Varandas and S. J. Formosinho, J. Chem. Soc., Faraday Trans. 2 82, 953 (1986).
6. S. J. Formosinho. J. Chem. Soc., Perkin Trans. 2 839 (1988)
7. (a) S. J. Formosinho, J. Chem. Soc., Perkin Trans. 2 61 (1987); (b) S. J. Formosinho and V. M. S. Gil, J. Chem. Soc., Perkin Trans. 2 1655 (1987).
8. L. G. Arnaut and S. J. Formosinho, J. Phys. Chem. 92, 685 (1988).
9. S. J. Formosinho, Tetrahedron 43, 1109 (1987).
10. S. J. Formosinho, Tetrahedron 42, 4557 (1986).
11. H. D. Burrows and S. J. Formosinho, J. Chem. Soc., Faraday Trans. 2 82, 1563 (1986).
12. S. J. Formosinho and A. J. C. Varandas, Mem. Acad. Ciênc. Lisboa, in press.
13. R. A. More O'Ferrall, J. Chem. Soc. B 274 (1970); W. J. Albery and M. M. Kreevoy, Adv. Phys. Org. Chem. 16, 87 (1978); E. R. Thornton, J. Am. Chem. Soc. 89, 2915 (1967); D. A. Jencks and W. P. J. Jencks, J. Am. Chem. Soc. 99, 7948 (1977); M. M. Kreevoy and D. E. Konasewich, J. Am. Chem. Soc. 74, 4464 (1970); J. R. Murdoch, J. Am. Chem. Soc. 105, 2667 (1983); E. Grunwald J. Am. Chem. Soc. 107, 125. (1985).
14. S. J. Formosinho, Rev. Port. Quim. 28, 61 (1986).
15. A. J. Gordon and R. A. Ford, The Chemist's Companion, pp. 107 and 114. Wiley, New York (1972).
16. M. A. El-Bayoumi and O. S. Khalil, J. Chem. Phys. 47, 4863 (1967).
17. F. Brogli, E. Heilbronner and T. Kobayashi, Helv. Chim. Acta 55, 274 (1972).
18. R. C. Weast (ed.) Handbook of Chemistry and Physics, 53rd ed., E-63. CRC Press, Cleveland, OH (1972).
19. L. G. Arnaut and S. J. Formosinho, J. Phys. Org. Chem. 3, 95–109 (1990).
20. C. G. Swain, R. A. Wiles and R. F. W. Bader, J. Am. Chem. Soc. 83, 1945 (1961); E. S. Lewis and M. C. R. Symons, Q. Rev. Chem. Soc. 12, 230 (1958).
21. S. J. Formosinho, Pure Appl. Chem. 58, 1173 (1986); L. G. Arnaut and S. J. Formosinho, J. Photochem. 39, 13 (1987); L. G. Arnaut and S. J. Formosinho, Adv. Photochem. in press.
22. S. J. Formosinho, J. Chem. Soc., Faraday Trans. 2 72, 1313 (1976); 74, 1978 (1978)
23. S. G. Lias, D. M. Shold and P. Ausloos, J. Am. Chem. Soc. 102, 2540 (1980).